

Effect of Secondary Lens Concentrators on the Output Parameters of Solar Modules with Cascade Photovoltaic Converters

N. Yu. Davidyuk, E. A. Ionova, D. A. Malevskii,
V. D. Rumyantsev, and N. A. Sadchikov

Ioffe Physical–Technical Institute, Russian Academy of Sciences, Politekhnicheskaya ul. 26, St. Petersburg, 194021 Russia
e-mail: vmandreev@mail.ioffe.ru

Received September 15, 2009

Abstract—The feasibility of increasing the concentration ratio and expanding the misorientation curve using secondary lens elements is considered for solar modules with triple-junction InGaP/GaAs/Ge photovoltaic converters and radiation-concentrating Fresnel lenses. Composite glass–silicone Fresnel lenses measuring 40×40 and 60×60 mm (plan view) with focal lengths of 70 and 110 mm, respectively, are used as primary concentrators. The focal length of secondary plane-convex glass lenses is varied from 5 to 25 mm. With the shortest-focal-length secondary lenses used, measurements of the parameters of the photovoltaic converter in a system with radiation concentrators that were made with a pulsed solar tester show the increase in the concentration ratio and the expansion of the misorientation curve by a factor of 2.5–3.0. The parameters of test modules with lens panels measured under solar illumination are found to be in good agreement with laboratory data.

DOI: 10.1134/S1063784210070145

INTRODUCTION

“Novel power engineering,” which is based on wide utilization of solar energy, is aimed at diminishing the reliance of the world community on fossil (organic and nuclear) fuels. Direct solar-to-electric energy conversion by means of efficient nanoheterostructure III–V solar cells (SCs) seems to be the most promising approach in this respect [1, 2]. An efficiency as high as 39–41% in triple-junction (Al)GaInP/Ga(In)As/Ge monocrystalline SCs in which three photoactive p – n junctions are integrated (series-connected) in one chip (with prospects for raising the efficiency up to 50% in structures with a larger number of stages) has been reported [3–5]. The economic effect of using such SCs is provided owing to cheap optical concentrators of solar radiation.

Composite Fresnel lenses in which the front region represents a sheet of normal silicate glass the inner surface of which serving as a substrate accommodates a concentric set of refractive microlenses made of a transparent silicone compound are today viewed as an inviting prospect [6, 7]. Since the rise in the concentration ratio is intimately related to the chip’s real estate saving, the rise in the ratio averaged over the chip’s surface area reduces the partial SC cost in the total cost of unit power from a solar plant. It is remembered that the SC operation at a high photocurrent density is also preferable when it comes to achieving ultimate efficiency [8].

For the conversion of concentrated solar radiation to be efficient, it is necessary that a concentrator–SC

system keep track of the position of the sun in the sky. The higher the concentration ratio, the higher the tracking accuracy. However, one can constrict the solar spot on the SC surface by locally increasing the concentration ratio and thereby allowing the displacement of the spot within the light-sensitive area without decreasing the output power. In this way, the range of misorientation angles can be extended and the requirements on the tracking accuracy can be reduced. Thus, the SC operation at high light flux density is desirable as far as the physics of the process and the cost efficiency and design of photovoltaic conversion systems are concerned.

It should be noted that the solar concentration ratio in a concentrator–SC system is limited. Limitations depend on the focusing force of Fresnel lenses and on the ability of the SC design to minimize the inner electrical resistance and withstand thermal loads. A secondary optical element added to the optical scheme of a photovoltaic system may considerably improve its performance. Usually, conic reflectors are used as secondary elements. They are made from polished aluminum sheet or glass block with polished lateral surfaces [9–11]. In the latter case, the effect of total internal reflection at the glass–air interface is used. The disadvantages of conic reflectors are limited concentration ratio and the need to mount them in the neighborhood of the SC: by providing a very narrow gap in the case of hollow aluminum reflectors or an optical contact (using an appropriate adhesive compound) in the case of glass reflectors.

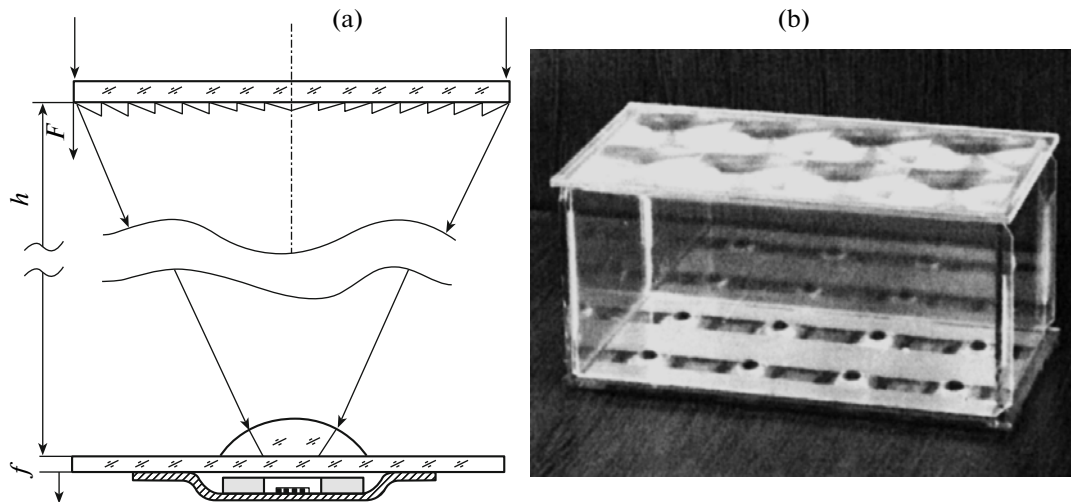


Fig. 1. (a) Optical scheme of the unit concentrator solar module. Shown are the planes from which the focal lengths of the primary Fresnel lens (F) and secondary lens (f) are measured and distance h between the front and rear bases of the modules. (b) Photo of a module with nanoheterostructure SCs and secondary lenses that is designed for field tests (FL60-based eight-lens module with glass side walls).

One can apply small plane-convex lenses as secondary optical elements. Such lenses, placed at a distance from the SC surface, focus the radiation from the primary Fresnel lens [6, 11]. The aim of this work is gaining a deep insight into the effect of secondary lens concentrators on the output parameters of solar modules including primary Fresnel lenses and efficient triple-junction SCs.

OPTICAL SCHEME OF CONCENTRATOR SOLAR MODULES

Figure 1 shows the optical scheme of a unit module in which composite Fresnel lenses and a small plane-convex lens serve as primary concentrators and a secondary concentrator, respectively. A SC is mounted on a copper heatsink, which, in turn, is placed on the outer surface of the rear glass base of the module. To protect the module against environmental action, a thin air gap between the shaped heat-spreading plate and the glass base is sealed. The small plane-convex lens is glued on the inner surface of the rear base of the module in front of the SC. The composite glass–silicone Fresnel lenses have a square shape measuring in plan view either 40×40 mm (hereinafter FL40) or 60×60 mm (FL60). Focal length F of the primary lenses measured from the inner surface of their glass substrate was equal to 70 and 110 mm, respectively. The diameter of the photosensitive area of the SC equaled 1.7 mm for the smaller lenses and 2.3 mm for the larger ones.

In laboratory experiments using a solar tester, focal length f of the secondary plane-convex glass lens was varied from 5 to 25 mm and distance h between the front and rear bases of the module was varied with an adjustment gear on a mechanical support. From the

results of these experiments, we prepared unit and multiple-Fresnel-lens test modules (Fig. 1b) intended for field tests under solar illumination.

MEASURING TECHNIQUE

Laboratory experiments with unit concentration modules were conducted using the original solar tester comprising a pulsed light source (xenon lamp), a collimator, and a measuring block [12]. The tubular glowing region of the lamp was covered by a light-impermeable shield with a hole 6 mm in diameter. The hole was at the focal point of an aberration-free reflecting objective. The focal distance of the objective was larger than the diameter of the hole 100-fold, so that the residual divergence of the collimated radiation corresponded to the divergence of sun rays ($32'$). The radiation spectrum of the lamp was corrected by an interference filter so as to meet the AM 1.5 solar spectrum.

The power density of the pulsed radiation having passed through the collimator was set equal to 850 W/cm^2 . The concentrator photovoltaical system (Fresnel lens–secondary lens–SC with heatsink) was mounted on mechanical adjustment gears making it possible to align the elements, control the distance between them, and provide transverse rotation of the whole system about the optical axis of the collimator.

A triple-junction InGaP/GaAs/Ge SC was soldered to the shaped heat-spreading plate, which, in turn, was mounted in the immediate vicinity of the rear glass base of the module with a 0.5-mm gap between the glass and SC. The SC was connected to the measuring unit of the tester. The power supply of the lamp, measuring unit, and mechanical gears were controlled with a computer.

The xenon lamp generated 1-ms-long flat light pulses. The pulse repetition period was 10–15 s. Within the flat part of the pulse, a sweep voltage was applied to the SC to take an illuminated $I-V$ characteristic. A data acquisition system recorded the parameters of the $I-V$ curve, such as the short-circuit current (I_{sc}), output power at the optimal illuminated point (P_{max}), fill factor (FF) of the characteristic, and photovoltaic conversion efficiency. In a number of experiments, a misorientation curve of the module, that is, the dependence of current I_{sc} on the angle between the optical axes of the module and collimator, was constructed. The permissible range of the radiation acceptance angle was estimated from the half-width of this curve at a level of 0.9 ($\pm W_{0.9}$) under normal incidence of sun rays on the primary lens. Also, we made photometric measurements of the light spot on the SC surface. To do this, the SC was replaced by a single-junction GaAs photodetector with a diaphragm 0.12 mm in diameter. Special calibration allowed us to determine the absolute value of the local radiation concentration ratio and estimate the diameter of the spot from the value of 0.1 of the maximal photocurrent at the center ($d_{0.1}$).

The photovoltaic parameters of the test modules under field conditions were measured with the modules placed on the sun-tracking system. Illuminated $I-V$ curves were recorded using an analog-to-digital measuring unit, and the power density of direct solar radiation was measured with a Kipp and Zoned CH-1 calibrated pyrhelimeter and a solar cell calibrated in the National Renewable Energy Laboratory (Golden, Colorado, United States).

RESULTS OF LABORATORY EXPERIMENTS

At the first stage of investigation, we selected optimal distance h for each pair of primary and secondary lenses (taken from a prepared set, see below) incorporated into a module. As the optimization criterion, we chose maximization of the photovoltaic conversion

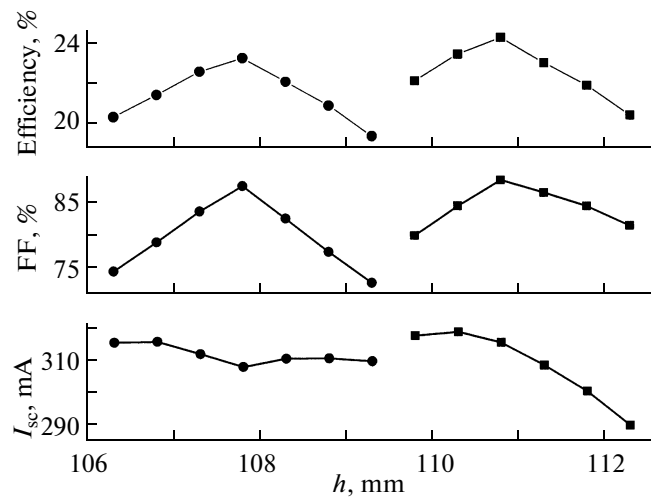


Fig. 2. I_{sc} , FF, and conversion efficiency vs. distance h for an FL60 in combination with the SC 2.3 mm in diameter. The curves on the right are depicted for the case when secondary optical elements are absent, and those on the left refer to the case when a secondary lens with focal length $f=8$ mm is introduced.

efficiency (note that the efficiency may both increase with varying distance because of better focusing and decrease because of a too high local concentration of radiation, which causes the FF in the illuminated $I-V$ curve to decrease).

By way of example, Fig. 2 plots I_{sc} , FF, and efficiency versus distance h for an FL60 and a SC 2.3 mm in diameter. This figure also gives us an idea of the necessary accuracy of primary and secondary lens arrangement along the optical axis (this accuracy equals 0.25 mm).

Tables 1 and 2 list the parameters of the test unit modules measured under laboratory conditions with the solar tester. The following features are typical of the modules of both sizes. As expected, an intermediate rear glass introduced into the arrangement of secondary lenses reduces the current and efficiency as a result of light reflection at two additional glass–air

Table 1. Parameters of the unit module with FL40 and SC 1.7 mm in diameter

Output parameters and experimental conditions	I_{sc} , mA	FF, %	P_{max} , mW	Efficiency, %	$d_{0.1}$, mm	C_{max} , factor	$\pm W_{0.9}^\circ$
Primary Fresnel lens and SC without rear glass	141	86.9	382	23.8	1.15	1732	
Same with rear glass and without secondary lens	127	87.7	348	21.8			0.35
Secondary lens $f=25$ mm with antireflection coating on convex side	135	87.9	376	22.9	0.98	1880	0.47
Same, $f=20$ mm	135	87.2	366	22.8			0.49
Same, $f=8$ mm, without antireflection coating	133	85.8	354	22.0	0.73	4240	0.71
Same, $f=5$ mm, without antireflection coating	129	86.1	343	21.5	0.56	6826	1.0

Table 2. Parameters of the unit module with FL60 and SC 2.3 mm in diameter

Output parameters and experimental conditions	I_{sc} , mA	FF, %	P_{max} , mW	Efficiency, %	$d_{0.1}$, mm	C_{max} , factor	$\pm W_{0.9}^{\circ}$
Primary Fresnel lens and SC without rear glass	316	88.1	870	24.2	1.84	1640	
Same with rear glass and without secondary lens	291	86.6	784	21.7			0.257
Secondary lens $f = 25$ mm with antireflection coating on convex side	310	86.1	832	23.2	1.56	2226	0.367
Same, $f = 20$ mm	312	85.9	834	23.0			0.374
Same, $f = 8$ mm, without antireflection coating	308	87.2	839	23.2	1.12	4320	0.587
Same, $f = 5$ mm, without antireflection coating	303	85.5	808	22.5	1.0	6960	0.900

interfaces. The introduction of long-focus secondary lenses with a one-sided antireflection coating raises the current through a partial decrease in the reflection and a better collection of the light on the SC surface.

In the case of short-focus secondary lenses, the current to a great extent recovers even in the absence of antireflection coatings. This takes place outright thanks to focusing of the radiation. A positive fact here is that the FF of the $I-V$ curve was always higher than 85% despite the considerable decrease in the light spot diameter and its corresponding increase in the local concentration ratio of radiation.

When the optical axis of the module is offset from the axis of the radiation source, a smaller light spot

may stay on the SC surface for a longer time. That is why the misorientation characteristic of the modules expands threefold in the case of the shortest-focal-length lenses. From Tables 1 and 2, it follows that the set of parameters of secondary lenses with $f = 8$ mm is optimal for application in the modules of both sizes.

RESULTS OF FIELD EXPERIMENTS

Field measurements under solar illumination were made for unit and multilens concentrator modules without secondary lenses (reference modules) and for modules with secondary lenses (focal length $f = 8$ mm). Figure 3 shows the illuminated $I-V$ curves of the unit module with FL40 and the SC 1.7 mm in diameter under illumination by sun rays incident normally to the front surface of the module. The dashed line refers to the module without the secondary lens. Since this module incorporates the best examples of the primary Fresnel lens and SC, its efficiency is as high as 27.1%. The continuous curve in Fig. 3 refers to the case when the secondary lens with $f = 8$ mm is introduced. Here, the efficiency is somewhat lower, 25.7%. The decrease in the efficiency by 1.4% is due to the reflection from two additional glass faces. It can be completely compensated for with the help of antireflection coatings.

Figure 4 demonstrates misorientation curves (the dependences of the short-circuit current on the angle between the optical axis of the module and the direction toward the Sun) for the same module with and without the secondary lens. The secondary lens is seen to increase the half-width of the curve at a level of 0.9, $\pm W_{0.9}$, from $\pm 0.39^{\circ}$ to $\pm 0.72^{\circ}$.

Figure 5 shows the illuminated $I-V$ curve for the eight-lens (FL60) module with the SC 2.3 mm in diameter and secondary lenses with $f = 8$ mm (see Fig. 1). Solar radiation was incident normally to the front surface. For an incident radiation power density of 901 W/cm^2 , the efficiency of the module was equal to 21.4%. The ambient temperature was 24°C , while the temperature of the SC was estimated as $42\text{--}45^{\circ}\text{C}$; that

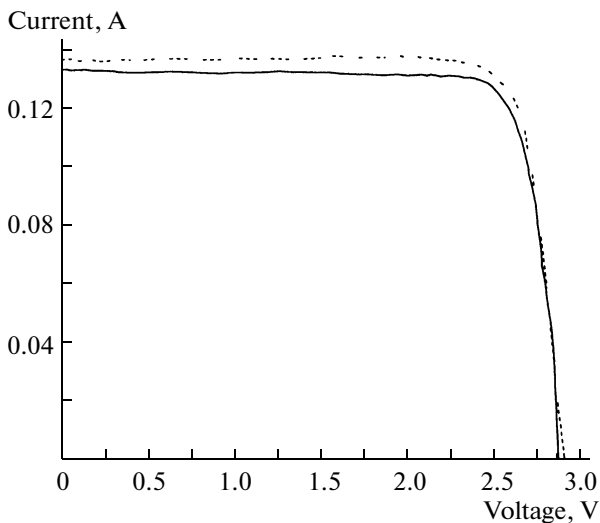


Fig. 3. Illuminated $I-V$ curves of the unit module with the FL40 and SC 1.7 mm in diameter under solar illumination. The dashed line refers to the case when the secondary lens is absent, power density E of incident solar radiation is 786 W/cm^2 , and the efficiency of the module is 27.1%. The continuous curve refers to the case when the secondary lens with $f = 8$ mm is introduced, $E = 790 \text{ W/cm}^2$, and the efficiency of the module is 25.7%. The ambient temperature is 22°C . The values of the efficiency are not corrected to the increased temperature of the SC.

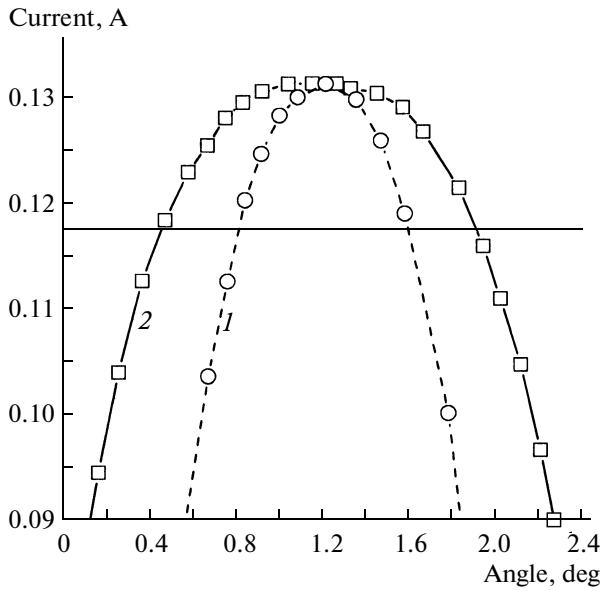


Fig. 4. Misorientation curves for the FL40-based module with the SC 1.7 mm in diameter under solar illumination (1) without the secondary lens, $\pm W_{0.9} = \pm 0.39^\circ$, and (2) with the secondary lens ($f = 8$ mm), $\pm W_{0.9} = \pm 0.72^\circ$.

is, the temperature of the converter was much higher than a standard value of 25°C , at which the results of such measurements are usually compared. The performance of this module displaced from the direction toward the Sun was compared with that of the same module without secondary lenses (see Fig. 6). As in the previous case, secondary lenses provide a considerable expansion of the area under the misorientation curve; namely, $\pm W_{0.9}$ changes from $\pm 0.27^\circ$ to $\pm 0.64^\circ$.

CONCLUSIONS

Laboratory and field tests of concentrator solar modules with secondary lens elements and nanoheterostructure cascade photovoltaic converters showed that such a design offers the following advantages.

Since the focal spot is smaller, the range of angles of solar radiation acceptance by the module extends with the SC dimensions being the same; alternatively, one can use smaller SCs.

There arises the possibility of protecting the SC against detrimental environmental actions (dust, condensate) by sealing a narrow air gap formed by an additional secondary-lens glass panel.

Finally, secondary lens elements are easy to mount; specifically, no direct contact with the photosensitive area of the SC is required. This makes it possible to eliminate problems associated with the placement of reflecting secondary elements (the need for a very narrow gap which may stimulate corrosion interaction with the SC in the case of metallic reflectors or the need for an adhesive optical contact and its possible radiation damage in the case of glass elements based

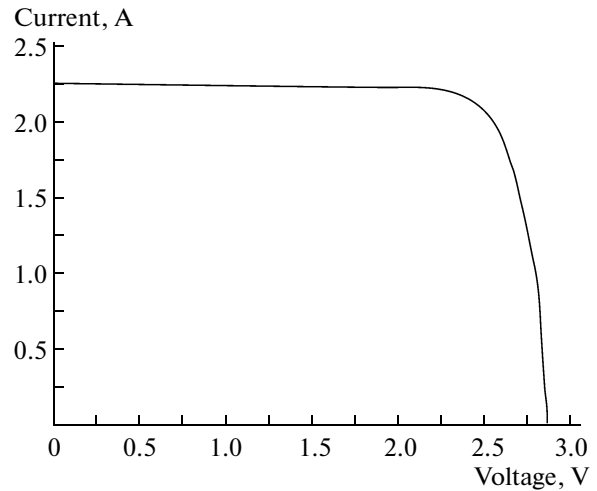


Fig. 5. Illuminated I - V curve of the eight-lens module with FL60, SC 2.3 mm in diameter, and secondary lenses with $f = 8$ mm under solar illumination. The power density of the incident solar radiation is 901 W/cm^2 , the conversion efficiency is 21.4%, and the ambient temperature is 24°C . The value of the efficiency is not corrected to the increased temperature of the SC.

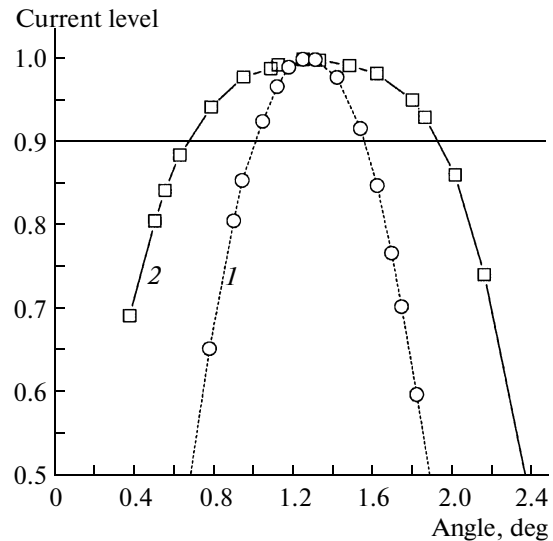


Fig. 6. Misorientation curves under solar illumination for two eight-lens modules with FL60 and SC 2.3 mm in diameter (1) without secondary lenses ($\pm W_{0.9} = \pm 0.27^\circ$) and (2) with secondary lenses with $f = 8$ mm ($\pm W_{0.9} = \pm 0.64^\circ$).

on the principle of total internal reflection). Minor optical losses due to the introduction of secondary lenses can be partially compensated for by using anti-reflection coatings. In this case, one can gain even an absolute rise in the efficiency owing to a better collection of light in a two-lens concentrator system.

Our further efforts will go into designing equipment and necessary attachments for precision mounting of the components in full-size concentrator modules.

ACKNOWLEDGMENTS

This work was supported by the Russian Foundation for Basic Research, grant no. 09-08-00412-a.

REFERENCES

1. Zh. I. Alferov, V. M. Andreev, and V. D. Romyantsev, *Fiz. Tekh. Poluprovodn. (St. Petersburg)* **38**, 937 (2004) [*Semiconductors* **38**, 899 (2004)].
2. Zh. I. Alferov, V. M. Andreev, and V. D. Romyantsev, *High-Efficient Low-Cost Photovoltaics*, Springer Ser. Opt. Sci. **140**, 101 (2008).
3. N. H. Karam, R. A. Sherif, and R. R. King, *High-Efficient Low-Cost Photovoltaics*, Springer Ser. Opt. Sci. **140**, 199 (2008).
4. A. W. Bett, F. Dimroth, and G. Siefer, *High-Efficient Low-Cost Photovoltaics*, Springer Ser. Opt. Sci. **140**, 67 (2008).
5. V. M. Andreev, V. D. Romyantsev, V. M. Lantratov, M. Z. Shvarts, N. A. Kalyuzhnyi, and S. A. Mintairov, in *Proceedings of the International Forum on Nanotechnology, Moscow, 2008*, Vol. 1, pp. 360–362.
6. V. D. Romyantsev, O. I. Chosta, V. A. Grilikhes, N. A. Sadchikov, A. A. Soluyanov, M. Z. Shvarts, and V. M. Andreev, in *Proceedings of the 29th IEEE Photovoltaic Specialists Conference (PVSC), 2002, New Orleans*, pp. 1596–1599.
7. V. D. Romyantsev, *Concentrator Photovoltaics*, Springer Ser. Opt. Sci. **130**, 151 (2007).
8. V. M. Andreev, V. A. Grilikhes, and V. D. Romyantsev, *Photovoltaic Conversion of Concentrated Solar Radiation* (Nauka, Leningrad, 1989) [in Russian].
9. K. Araki, M. Kondo, H. Uozumi, and M. Yamaguchi, in *Proceedings of the 3rd World Conference on Photovoltaic and Energy Conversion, Osaka, 2003*, pp. 853–856.
10. J. Jaus, P. Nitz, G. Peharz, G. Siefer, T. Schult, O. Wolf, M. Passig, T. Gandy, and A. W. Bett, in *Proceedings of the 33rd IEEE Photovoltaic Specialists Conference, San Diego, 2008*.
11. V. D. Romyantsev, N. Yu. Davidiyuk, E. A. Ionova, V. R. Larionov, D. A. Malevskiy, P. V. Pokrovskiy, N. A. Sadchikov, and V. M. Andreev, in *Proceedings of the 5th International Conference on Solar Concentrators for the Generation of Electricity, Palm Desert, 2008* (Proceedings on CD).
12. V. M. Andreev, V. R. Larionov, I. V. Lovygin, D. A. Malevskii, M. Ya. Maslenkov, V. D. Romyantsev, and M. Z. Shvarts, in *Proceedings of the International Forum on Nanotechnology, Moscow, 2008*, Vol. 1, pp. 205–207.